

## Post-processing improves accuracy of Artificial Intelligence weather forecasts

BELINDA TROTTA<sup>a</sup>, ROBERT JOHNSON<sup>a</sup>, CATHERINE DE BURGH-DAY<sup>a</sup>, DEBRA HUDSON<sup>a</sup>, ESTEBAN ABELLAN<sup>a</sup>, JAMES CANVIN<sup>a</sup>, ANDREW KELLY<sup>a</sup>, DANIEL MENTIPLAY<sup>a</sup>, BENJAMIN OWEN<sup>a</sup>, JENNIFER WHELAN<sup>a</sup>

<sup>a</sup> *Bureau of Meteorology, Australia*

**ABSTRACT:** Artificial Intelligence (AI) weather models are now reaching operational-grade performance for some variables, but like traditional Numerical Weather Prediction (NWP) models, they exhibit systematic biases and reliability issues. We test the application of the Bureau of Meteorology’s existing statistical post-processing system, IMPROVER, to ECMWF’s deterministic Artificial Intelligence Forecasting System (AIFS), and compare results against post-processed outputs from the ECMWF HRES and ENS models. Without any modification to configuration or processing workflows, post-processing yields comparable accuracy improvements for AIFS as for traditional NWP forecasts, in both expected value and probabilistic outputs. We show that blending AIFS with NWP models improves overall forecast skill, even when AIFS alone is not the most accurate component. These findings show that statistical post-processing methods developed for NWP are directly applicable to AI models, enabling national meteorological centres to incorporate AI forecasts into existing workflows in a low-risk, incremental fashion.

### Notice

This Work has been submitted to Artificial Intelligence for the Earth Systems. Copyright in this Work may be transferred without further notice.

### 1. Introduction

Artificial Intelligence weather models have rapidly improved in the last few years (de Burgh-Day and Leeuwenburg 2023). Deterministic AI models now typically achieve RMSE accuracy as good or better than traditional Numerical Weather Prediction (NWP) models for medium-range forecasting on most variables assessed, while being many times faster to run. In this study, we focus on the European Centre for Medium-Range Weather Forecasting’s (ECMWF) deterministic Artificial Intelligence Forecasting System (AIFS) model (Lang et al. 2024a), which is operationally supported as of 25 February 2025 (ECMWF 2025b). AIFS is a graph transformer neural network. Graph-based architectures have been hugely successful in weather modelling. Deepmind’s GraphCast model was found to have better RMSE skill score than ECMWF’s HRES deterministic model in around 90% of cases (Lam et al. 2023). Like GraphCast, AIFS generally outperforms HRES (Lang et al. 2024a). Earlier work by Keisler (2022) used a much smaller graph-based network and achieved results better than the Global Forecasting System (GFS, produced by the US National Oceanic and Atmospheric Administration) but not as good as the ECMWF’s HRES model.

As is the case for traditional NWP models, the resolution of AI weather models is limited by computational constraints. The resolution of AIFS is approximately 0.25°

(Lang et al. 2024a), significantly coarser than the 0.1° resolution of ECMWF HRES (ECMWF 2025a). Also, as discussed in section 4, AI models, and graph-based models in particular, tend to produce gridded outputs that are spatially very smooth. For these reasons, AI models can have difficulty modelling small-scale phenomena. Furthermore, the graph-based models described above are all auto-regressive: the first timestep is calculated by running the model on the current analysis, and then subsequent timesteps take as input the model output of the previous timestep. Therefore, it is expected that model errors can accumulate over time. Because of these limitations, we hypothesise that post-processing methods developed for NWP can be applied to AI forecasts without modification and yield comparable results, and that incorporating AI models into forecast blends will improve both deterministic and probabilistic forecast skill.

Since AI weather models have only recently become good enough to be considered for operational use, the study of post-processing such models is relatively undeveloped, compared to the large body of work on NWP models. However, existing research shows benefits from applying post-processing. Bremnes et al. (2024) use a neural network to produce calibrated probabilistic site forecasts of wind speed and temperature for the Pangu-Weather deterministic ML forecast (Bi et al. 2022), and apply the same methods to some deterministic and ensemble NWP forecasts. They find that post-processing yields large improvements in accuracy for both AI and NWP forecasts.

Bülte et al. (2025) evaluate two post-processing methods for producing probabilistic forecasts from Pangu-Weather, and compare the results with the ECMWF raw ensemble. In contrast to the work of Bremnes et al. (2024), the models are trained and evaluated on gridded analyses rather

---

Corresponding author: Belinda Trotta, belinda.trotta@bom.gov.au

than site data. The first method is the EasyUQ technique developed by Walz et al. (2024) and based on isotonic distributional regression of Henzi et al. (2021). This is a non-parametric non-AI calibration method somewhat similar to the reliability calibration used in the present work. The second method is distributional regression networks, an AI approach where post-processed forecasts follow parametric distributions whose parameters are predicted by a neural network based on the inputs. While the latter method allows incorporating additional predictors, it is found not to offer significant advantages over the simpler non-AI method. Both methods allow the post-processed deterministic forecast to achieve similar or better accuracy than the raw ECMWF ensemble, at least for the first few days of the forecast period. A much more sophisticated method is demonstrated by Ge et al. (2022), who use a deep neural network to bias correct and downscale gridded predictions to the point scale. Since the network has billions of parameters, training is computationally intensive and requires a long history of training data.

Here we apply the IMPROVER (Roberts et al. 2023) post-processing system to post-process the AIFS forecast outputs, and apply the same methods to ECMWF’s deterministic HRES and ensemble (ENS) models to provide a comparison. We demonstrate that although IMPROVER is developed for post-processing traditional NWP forecasts, it is also effective for AIFS with no changes to the configuration parameters or processing workflows. We also show that adding AIFS to a blend of models with the two traditional NWP forecasts improves the accuracy of the blend, even in situations where AIFS is less accurate than one of the other models. One of the key features of IMPROVER is that it facilitates producing probabilistic forecasts from both deterministic and ensemble NWP inputs. The probabilistic forecasts produced by AIFS are of comparable quality to those produced by ECMWF HRES and including AIFS in the blend improves the quality of the probabilistic forecast.

## 2. Data

The study uses data spanning 1 March 2024 to 23 July 2024 (with a few days of missing data, varying by parameter). The date range was limited by computational resources and the availability of archived pre-processed data. In future work, it would be interesting to consider a longer date range including the Summer period. AIFS data was downloaded from ECMWF’s Meteorological Archival and Retrieval System (MARS). Since calibration uses a rolling period of the previous 30 days of forecasts, the outputs are not reliable for the first month, and we analyse the results only from 1 April onwards, amounting to approximately 16 weeks of data. We consider forecasts from the 12Z base-time for each day in the period. We selected this basetime since, of the Bureau’s two daily operational forecasts, this

one receives the most attention. We post-process 3 surface-level variables: temperature, dew point temperature, and wind speed at 10m. We evaluate both the expected value and probabilistic output forecasts.

Post-processed forecasts are produced for lead times up to 240 hours at 1-hour intervals. The raw AIFS forecast has lead times at 6-hourly intervals, while the ENS and HRES forecasts have 3-hourly frequency up to 150 hours, and 6-hourly thereafter. The resolutions of the NWP forecasts ENS and HRES are  $0.2^\circ$  and  $0.1^\circ$ , respectively.<sup>1</sup> The AIFS forecast is produced on the N320 reduced Gaussian grid (see Lang et al. (2024a)). Our bias correction and calibration use the gridded analysis produced by Mesoscale Surface Analysis System (MSAS) (Glowacki et al. 2012), which has a resolution of 2.5 arc minutes (approximately 4 km on the Australian domain).

Hourly observation data was extracted from the Bureau of Meteorology’s Jive database (Loveday et al. 2024), which contains quality-controlled observations from the Bureau’s network of Automatic Weather Stations. In total, 569 weather stations are used in the analysis. Figure 1 shows the location of these stations.

## 3. Methods

AIFS data was pre-processed to a format expected by IMPROVER. As mentioned above, AIFS is produced on the N320 reduced Gaussian grid. The IMPROVER software cannot natively handle this grid, so as part of pre-processing we transform it to a latitude/longitude grid of resolution  $0.25^\circ$ . IMPROVER is already in use operationally at the Bureau of Meteorology for HRES, ENS, and MSAS, so for these models pre-processed data was retrieved from an operational archive.

IMPROVER produces probabilistic forecasts by predicting the probabilities of exceedence at a set of thresholds. Expected value forecasts were calculated from the probabilistic output by linearly interpolating these probabilities and integrating the resulting distribution.

The Bureau’s IMPROVER processing workflow is summarised in Section a and described in detail in (Owen et al. 2024) and (Owen et al. 2025). Forecast bias and probability calibration are corrected using a rolling history of 30 days of data. The ground truth for these corrections is the gridded MSAS analysis mentioned above. Probability calibration is implemented using the reliability calibration algorithm described by Flowerdew (2014).

After running the IMPROVER hindcast with AIFS, the output was extracted at the observation sites (Figure 1), and expected values were calculated from the thresholded forecast. For temperature, the expected value (but not the thresholded site forecast) was adjusted using the standard adiabatic lapse rate of  $-0.0098^\circ\text{C/m}$  to account for the

---

<sup>1</sup>ENS is produced by ECMWF at  $0.1^\circ$  resolution; the Bureau receives an upscaled version.

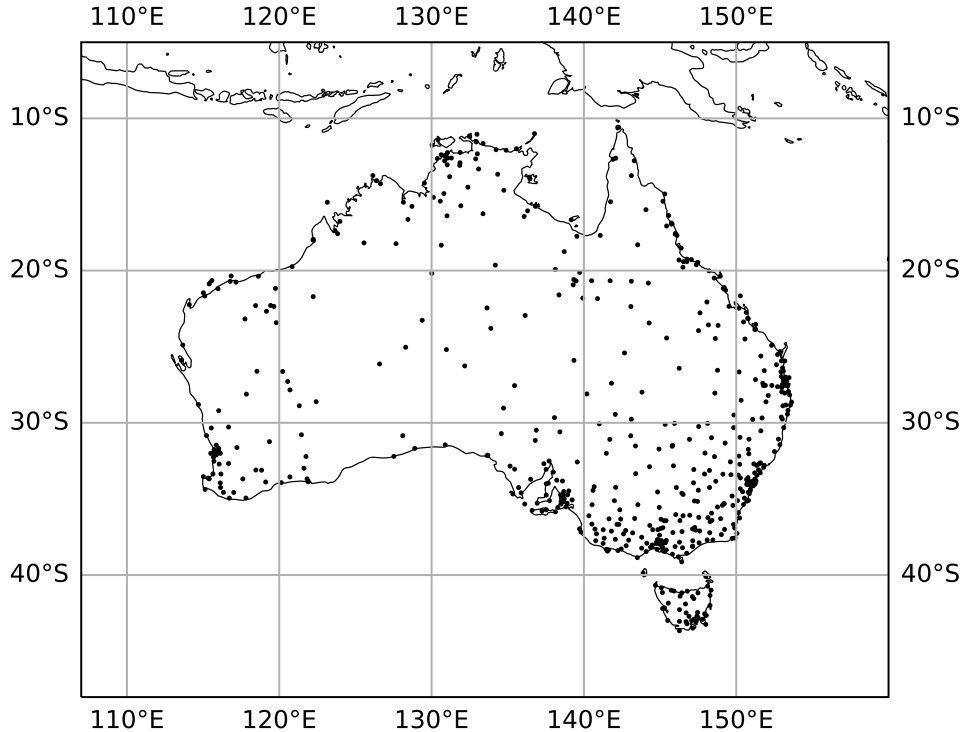


FIG. 1: The Australian continent, showing locations of the Bureau of Meteorology's Automatic Weather Stations used for verification in this study.

difference between the grid point average altitude and the site altitude.

As described in Section b, we created two blended forecasts using either the NWP models only, or the full set of models.

#### *a. IMPROVER processing*

Below we describe the main post-processing steps implemented by our IMPROVER operational configuration. More detail can be found in (Owen et al. 2024) and (Owen et al. 2025).

1. Linear interpolation from original lead times to hourly forecast.
2. Regridding to 2400m Albers equal area grid. (Note that this is in addition to the initial regridding of AIFS from the N320 grid as mentioned above.)
3. Gridded lapse rate correction (temperature forecast only). Since the grid of the raw forecast is different to the IMPROVER output grid, we apply a correction to

adjust for the difference between the average altitudes in each grid cell.

4. Bias correction (applied to each ensemble member in the case of ensemble forecasts). A separate correction is applied for each grid point and lead time, based on the previous 30 days' history of forecast bias. The historical forecasts are archived after the regridding step (or the lapse rate correction step, in the case of temperature). The ground truth for the correction is the gridded MSAS analysis. In the case of the ENS forecast, the bias is calculated from the ensemble mean forecast.
5. Thresholding (ensemble forecast) or fuzzy thresholding (deterministic forecast) to produce a probabilistic forecast. IMPROVER represents probabilistic forecasts as a set of probabilities and their corresponding probabilities of exceedence. For an ensemble forecast, thresholding simply means calculating the proportion of ensemble members that exceed the threshold. For a deterministic forecast, simple thresholding

would yield a probability of either 0 or 1, which is not useful for reliability calibration. Instead, we use the fuzzy thresholding approach, where the predicted value is mapped to a number between 0 and 1 depending how far it is from the threshold. See Owen et al. (2025) for more details on this technique.

6. Neighbourhood processing with 2500 m radius. This smooths the probabilistic forecast by convolving it with a constant-valued square filter.
7. Recursive filtering. An additional smoothing operation, similar to an exponential weighted average filter.
8. Reliability calibration. Probabilities are adjusted using a piecewise-linear correction function calculated as follows. For each threshold, the previous 30 days' history of forecasts are binned into 7 probability bins, and for each bin, the average forecast and observed probabilities of exceeding the threshold are calculated. The forecast and observed probabilities define the  $x$  and  $y$  coordinates, respectively, of the knot points of the piecewise linear correction function. The historical forecasts are archived after the thresholding step. Reliability calibration is calculated separately for each lead time, using the aggregate of all grid points. As is the case for bias correction, the MSAS analysis is used as ground truth.

#### *b. Blending weights*

We consider two blended forecasts: the first uses only the two NWP models, ENS and HRES, and the second uses all three models. In each case, the blending weights are chosen as follows. The data is split in half by valid time. Weights are fitted separately on each half of the data, and then applied to create the blended forecast for the other half of the data. Each set of weights is calculated as follows. First, we calculate the optimal weights at each lead time to minimise the mean squared error. However, these weights vary greatly from hour to hour, partly due to diurnal patterns in the model biases, and partly due to random noise. To reduce overfitting and improve generalisation, we calculate a second set of smoothed weights. The smoothed weight for each model is a piecewise-linear function of lead time with 11 knots at lead times 0, 24, 48, ... 240. The function values at the knot points are chosen to minimise the MSE between the piecewise linear function and the individual hourly optimal weights, then normalised to sum to 1 over all models at each knot point (which guarantees that the interpolated values between knot points also sum to 1).

Figure 2 shows the optimal weights when blending either all models, or only the two NWP models. (As described above, two sets of weights were fitted; the weights shown here are those fitted on the first half of the data.) For all

variables, AIFS contributes significantly to the blend, and for temperature and dew point, it is generally the main component in the early part of the forecast period.

## **4. Results**

As noted by Lang et al. (2024a) and Ben Bouall  gue et al. (2024), ML forecasts tend to have a smoother appearance than physics-based NWP, because they are based on optimising a loss function, which rewards predicting the middle of the distribution, rather than simulating physical processes. Additionally, graph neural networks, including the graph transformer architecture used in AIFS, are susceptible to a problem where, as the number of layers increases, message-passing between nodes increases similarity between the features of different nodes (Wu et al. 2023), which would contribute to visual smoothness of the gridded output. Figure 3 compares gridded HRES and AIFS temperature forecasts before and after post-processing. The input AIFS is noticeably smoother and less detailed than HRES, although this is partly also due also to their different resolutions,  $0.25^\circ$  vs  $0.1^\circ$ .<sup>2</sup> However, after post-processing, the outputs have a similar level of detail; in particular, it is worth noting that post-processing is able to add realistic topographic features.

Figure 4 shows forecast mean squared error by lead day before and after IMPROVER post-processing. For the raw ENS forecast, the quantity verified is the ensemble mean. Lead day 0 corresponds to lead hours 0-24 inclusive, lead day 1 to hours 25-48, et cetera. Post-processing generally improves the raw forecasts, yielding gains of a few days of skill in some cases. For all variables, the three post-processed models achieve similar accuracy early in the forecast period. For temperature and dew point, after the first few lead days AIFS has a clear advantage over HRES, with the gap widening as lead time increases.

It is well established that blending models generally improves the accuracy relative to the best individual forecast, and therefore it is a common approach in operational weather forecasts. Figure 5 compares the two different blends, along with the post-processed models. To measure the difference between the two blends, we used the Diebold-Mariano test to calculate a confidence interval for the difference in MSE for each lead day. This test requires that the time series of differences be weakly stationary. Therefore, in order to avoid diurnal and spatial biases in the error, for each lead time we aggregated the data by valid day and calculated the MSE (including all sites and

<sup>2</sup>For a comparison of AIFS vs the ECMWF integrated forecasting system (IFS) at the same resolution, see Figure 7 of Lang et al. (2024a). Similarly, Figure 3 in Ben Bouall  gue et al. (2024) compares the IFS with Pangu-Weather at equal resolution. In both examples, the AI forecasts are smoother than their NWP counterparts.

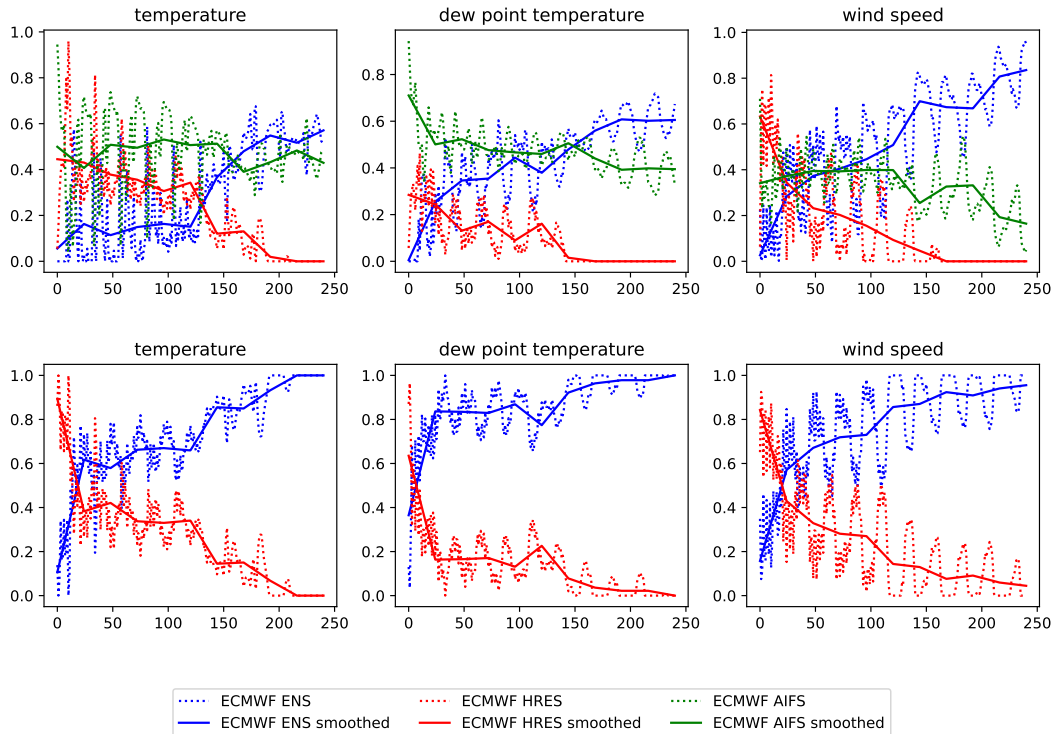


FIG. 2: Blending weights for all-model blend (top row) and NWP-model blend (ENS and HRES only; bottom row). The dotted line shows the optimal weights per lead hour. The solid line shows a smoothed version where a piecewise-linear function is fitted to the optimal weights.

valid times for that valid day).<sup>3</sup> The test statistic was calculated on this daily series, using the implementation in the “scores” Python package (Leeuwenburg et al. 2024) based on the method of Hering and Genton (2011). Figure 6 shows the MSE difference with confidence interval. Overall, the blend including all three models is significantly better than the blend of only the two NWP models.

Figure 7 shows the bias (defined as forecast minus observation) of the various models. As with MSE, for the raw ENS forecast, bias is calculated for the ensemble mean. Bias correction significantly mitigates the biases present in the raw forecasts. However some diurnal patterns and constant biases remain. This is to be expected because the IMPROVER bias correction is done relative to the MSAS analysis, which has its own biases relative to the observation data used for verification. We also observe trends in the bias over the forecast period. This is somewhat surpris-

ing, given that the bias correction and reliability calibration are calculated separately for each lead time. One possible explanation is that the calibration is based on a moving window of recent history, so at longer lead times there is a greater lag between the validity time of the forecast and the most recent ground truth used in the calibration. This perhaps reduces the ability of the calibration to correct for both seasonal model biases (that is, those varying systematically by time of year), and for idiosyncratic errors in the currently-occurring weather system.

IMPROVER produces probabilistic outputs individually for both deterministic and ensemble input forecasts. For evaluating their accuracy, we use the continuous ranked probability score (CRPS), which measures the error between the predicted probability distribution and the true outcome. The CRPS is defined as the integral of the squared distance between the forecast distribution and the true outcome; formally, if  $t \rightarrow P(X \leq t)$  is the predicted cumulative distribution function for some data point and  $x$

<sup>3</sup>The aggregation is slightly different from the aggregation by lead day shown in Figure 4, which simply combines all data for each lead day, without the intermediate step of taking the mean by valid day.

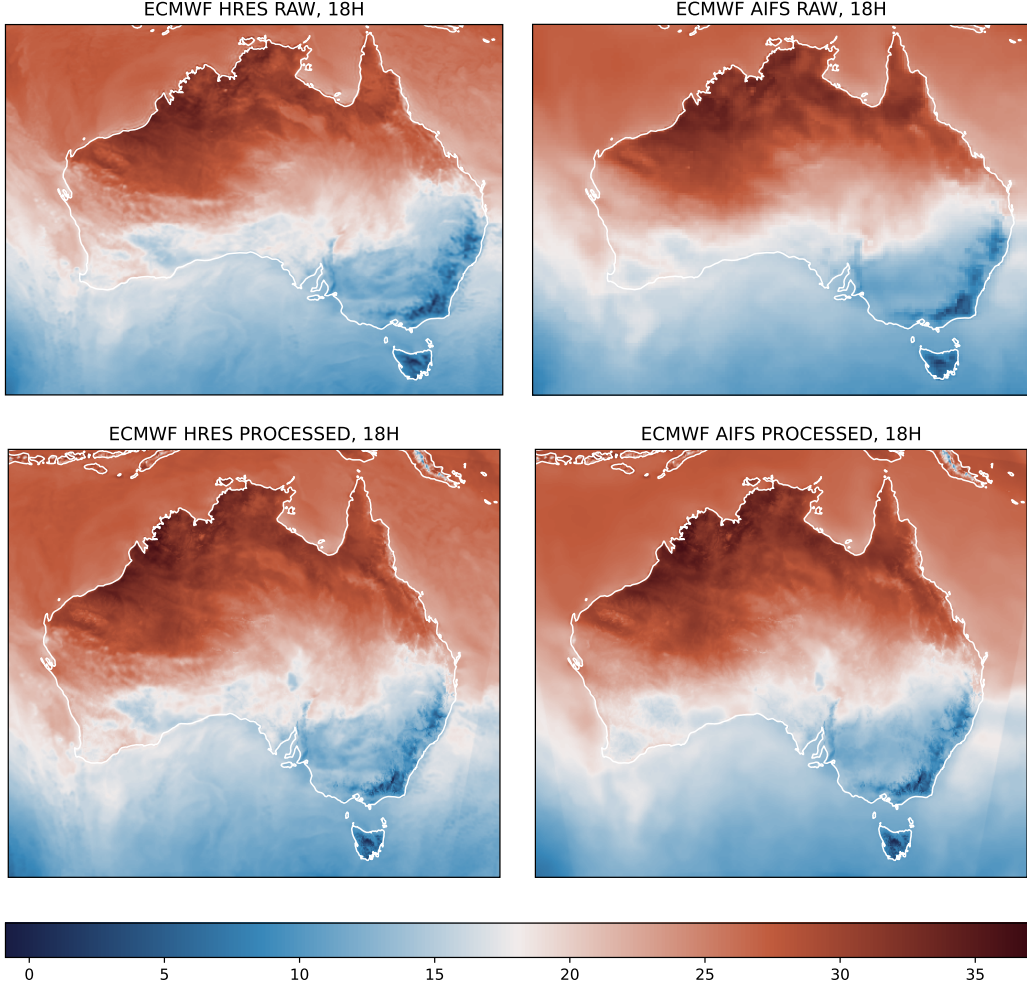


FIG. 3: Raw forecasts (top row) and post-processed expected value outputs from IMPROVER (bottom row) for temperature at lead time 18H and valid time 2024-06-15 06:00 UTC (16:00 Australian Eastern Standard Time). The left column is HRES and the right AIFS. Units are degrees Celsius. Note that the raw forecasts are on a latitude/longitude grid, while the post-processed forecasts use the Albers equal area projection. The diagonal artefacts near the edges in the lower part of the plots on the right occur because calibration is done against the MSAS analysis, which has a more limited spatial domain.

the observed value, the CRPS for this observation is

$$\int_{t=-\infty}^{t=\infty} \mathbb{P}(X \leq t) \mathbb{1}_{(t \geq x)} dt$$

where  $\mathbb{1}_{(t \geq x)}$  is the indicator function which is equal to 1 if  $t \geq x$  and 0 otherwise. Smaller CRPS values indicate a better forecast. Figure 8 shows the CRPS of the post-processed models and blends. While in general the blend of the two NWP models performs very similarly to the

most accurate individual NWP model, the blend of all three models yields a larger improvement. We used the Diebold-Mariano test to compare the two blends, following the same process as described above for the MSE comparison. The results are shown in Figure 9; as is the case with MSE, we see that the all-model blend is significantly better than the NWP-model blend.

Forecast reliability measures how well-calibrated a forecast is. Specifically, for a given threshold  $t$ , a forecast has

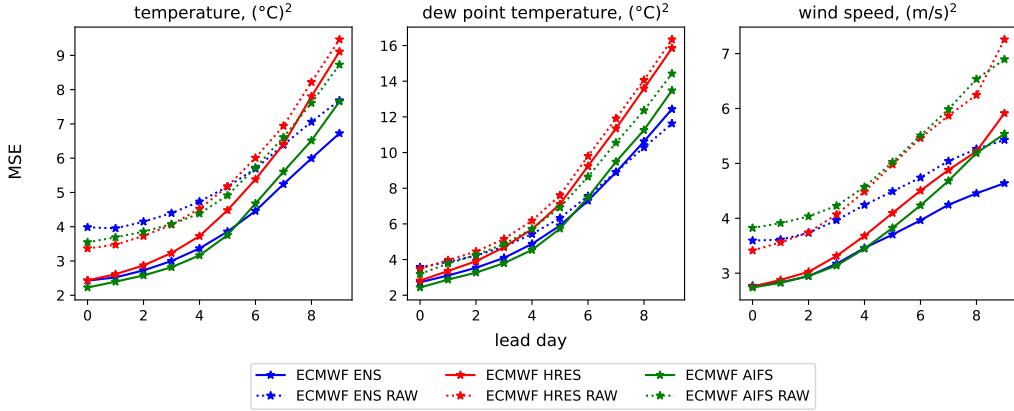


FIG. 4: Mean squared error by lead day for raw (dotted line) and post-processed (solid line) models ENS (blue), HRES (red) and AIFS (green), for temperature (left), dew point (middle) and wind speed (right). The calculation includes only lead times that are present in both the raw and post-processed forecasts (that is, those that are multiples of 6 hours).

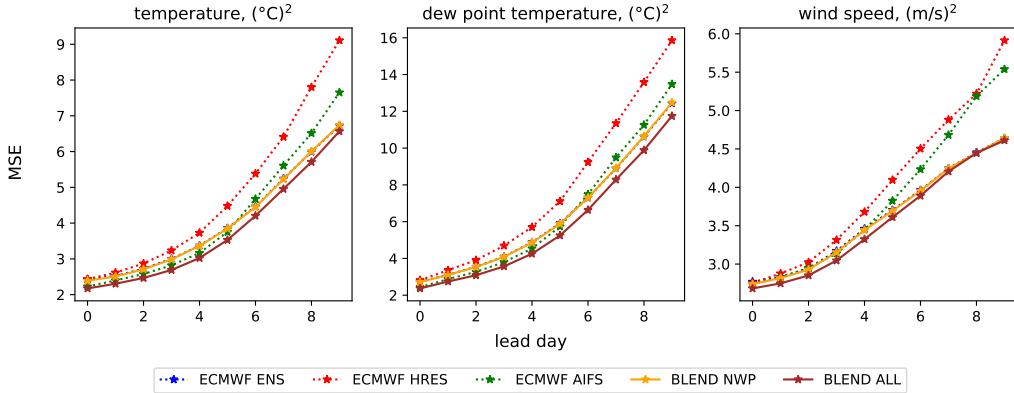


FIG. 5: Mean squared error by lead day for post-processed models ENS (blue), HRES (red) and AIFS (green) and blends (NWP models ENS and HRES, yellow; and all models, brown). Note that the line for ENS is very close to that of the NWP-model blend, and partially hidden by it.

good reliability if the conditional probability  $p_o$  that an observation exceeds  $t$ , given that the forecast probability is  $p_f$ , is approximately equal to  $p_f$ . Figure 10 shows the reliability at the 12-hour lead time (UTC 0) at selected thresholds, roughly corresponding to the 10th, 50th and 90th percentiles of the overall distribution of observations (including all times of day). There is no clear trend in these results: all models and blends have similar performance. The deterministic models arguably appear a little better than the ensemble, and the blended models do not seem to

offer much advantage. It has been shown by Ranjan and Gneiting (2010) that blending probability forecasts does not preserve calibration; that is, even if each individual forecast is perfectly calibrated, in general the blend is not. Therefore, calibration could likely be further improved by recalibrating the blend. Functionality to implement the parametric recalibration proposed by Ranjan and Gneiting has recently been implemented in the IMPROVER software library, but is not currently part of the IMPROVER operational system used for this work. In Figure 11 we



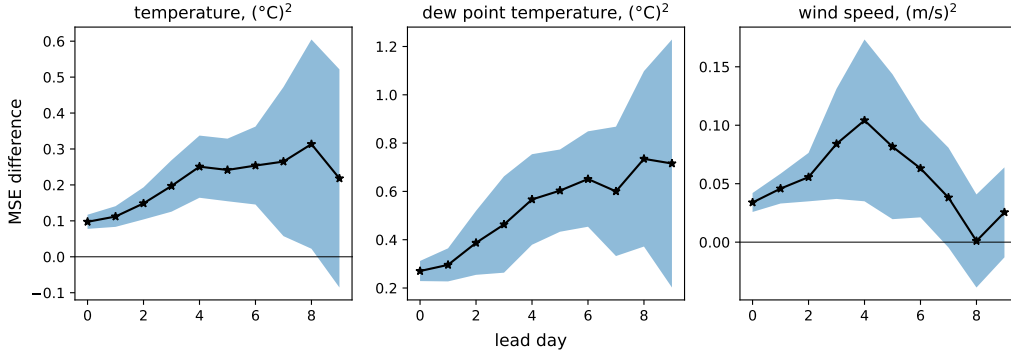


FIG. 6: MSE difference between NWP-model blend and all-model blend. The difference is  $\text{MSE}_{\text{NWP}} - \text{MSE}_{\text{all}}$ , so positive values indicate that the all-model blend is better. The shaded region is the 95% confidence interval.

show the distributions of probabilistic forecasts at this lead time. The 3-model blend is in general less sharp than the 2-model blend, which is in turn less sharp than the sharpest NWP model. Again, this is expected for blended forecasts, and could be corrected with recalibration.

## 5. Discussion

This study demonstrates that established statistical post-processing methods, originally designed for traditional Numerical Weather Prediction (NWP) models, are also effective when applied to forecasts from the Artificial Intelligence Forecasting System (AIFS). Using the Australian Bureau of Meteorology’s operational IMPROVER system without modification, we observe comparable accuracy improvements in AIFS forecasts to those seen with NWP models. Notably, blending AIFS with traditional NWP models yields consistent gains in forecast skill for both expected value and probabilistic forecasts. These results indicate that AI-based forecasts can be integrated into operational systems using existing tools and workflows, thereby expanding the utility of these forecasts without the need for bespoke post-processing solutions. A primary finding of this work is that statistical calibration via IMPROVER substantially improves the accuracy of AIFS forecasts. The gains are comparable to those achieved when calibrating traditional models, and in some cases, calibration adds upwards of a day of forecast skill. This reinforces our view that AI models, like their physics-based counterparts, benefit from correction of systematic errors using historical forecast performance. Importantly, the post-processing workflow required no changes, suggesting a high degree of generality in these methods.

The calibrated AIFS output also produces high-quality probabilistic forecasts. For temperature and dew point in

particular, the post-processed AIFS shows CRPS values similar to those of the ensemble system (ENS) during the early part of the forecast period. This is notable given that AIFS is a deterministic model, and the result highlights the value of fuzzy thresholding and reliability calibration in extracting probabilistic information from single-model inputs.

Visual inspection of gridded output shows that post-processing adds realistic spatial structure to AIFS forecasts, compensating for the low resolution of the raw model. This is achieved by bias correcting against the MSAS analysis, which has much finer raw resolution than AIFS, and, in the case of temperature, by lapse-rate adjustment to downscale to the finer grid. Our results demonstrate that statistical techniques can improve not only quantitative accuracy but also the visual detail of the forecast fields – an important element in operational weather forecasting.

The inclusion of AIFS in a blended forecast with NWP models consistently improves forecast accuracy across all variables (temperature, dew point, and wind speed). This result holds for both the deterministic mean squared error metric and probabilistic CRPS metric. The benefits of blending persist even when AIFS is individually less accurate than other models. This underscores the value of diversity in model formulation and suggests that AI models offer complementary strengths to traditional NWP models and enhance overall system performance when combined in this way.

These results provide a practical pathway for the adoption of AI-based weather forecasts by national meteorological centres. With AIFS now being officially supported by ECMWF, the demonstrated compatibility with existing post-processing systems means this forecast can be incorporated into current workflows without requiring customised infrastructure. Critically, blending allows for a



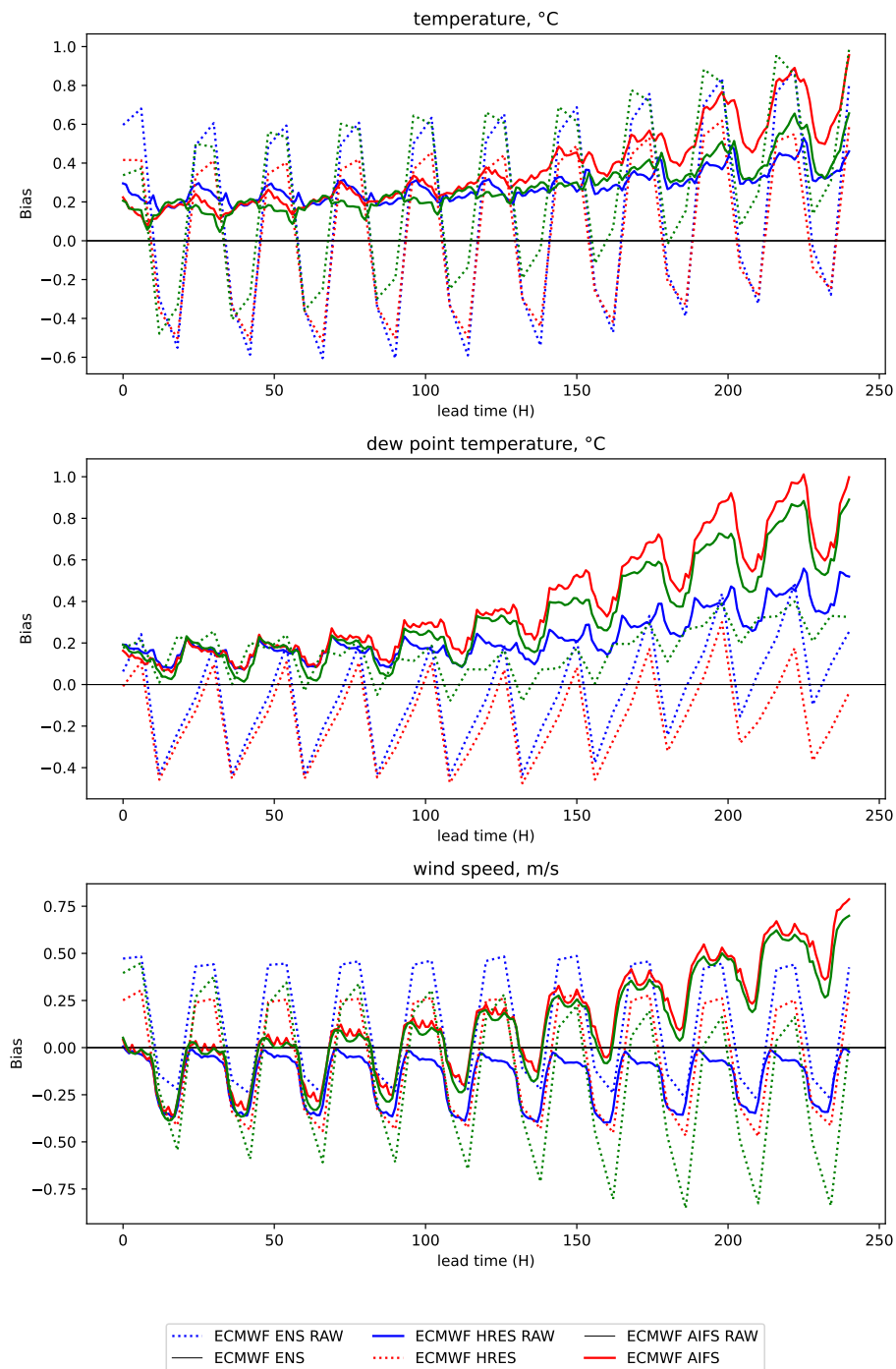


FIG. 7: Bias of raw (dashed line) and post-processed (solid line) models ENS (blue), HRES (red) and AIFS (green) over the forecast period. Note that the raw models have 6-hour lead time frequency, while the post-processed outputs have 1-hour frequency.

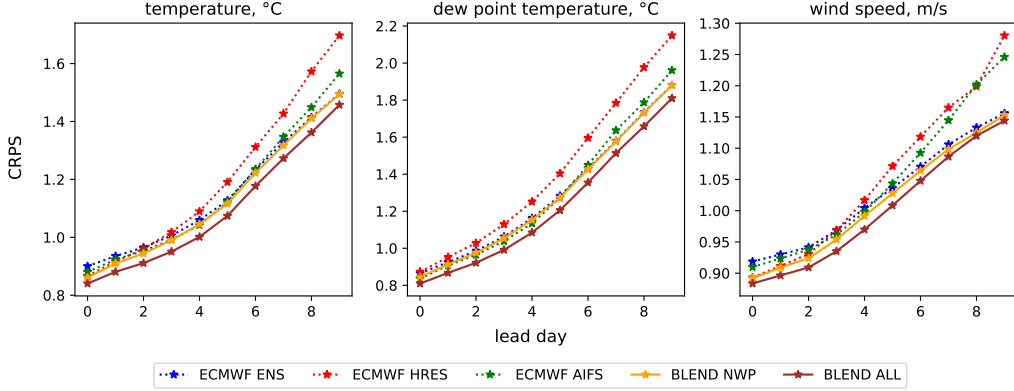


FIG. 8: Continuous rank probability score (CRPS) by lead day for post-processed models ENS (blue), HRES (red), and AIFS (green), and blends (NWP models ENS and HRES, yellow; and all models, brown) over the forecast period.

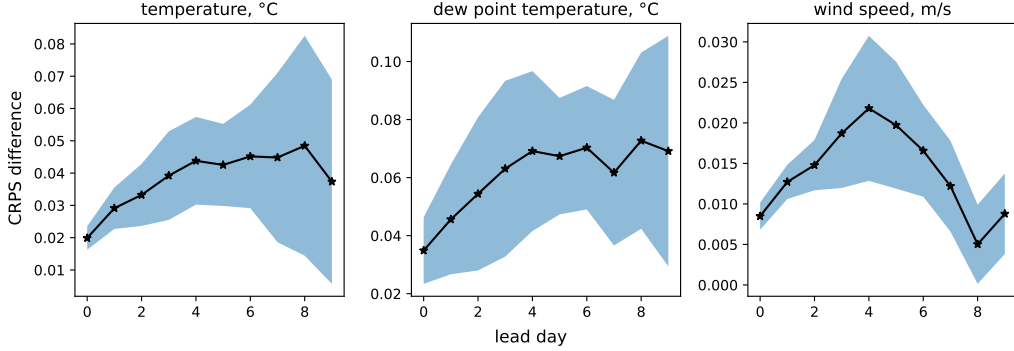


FIG. 9: CRPS difference between NWP-model blend and all-model blend. The difference is  $CRPS_{NWP} - CRPS_{all}$ , so positive values indicate that the all-model blend is better. The shaded region is the 95% confidence interval.

flexible, low-risk approach to operational use: rather than relying entirely on an AI model, centres can integrate it alongside traditional NWP models, assigning weights according to performance and risk tolerance. This incremental adoption strategy enables institutions to harness the benefits of AI innovation while maintaining forecast robustness and continuity.

Future work should consider extending these analyses to AIFS-CRPS (Lang et al. 2024b), an ensemble version of AIFS trained to minimise CRPS. This may further improve the skill of blended forecasts. Additionally, recalibrating the probabilistic blends – particularly in light of known issues with calibration preservation during blending – may yield further improvements.

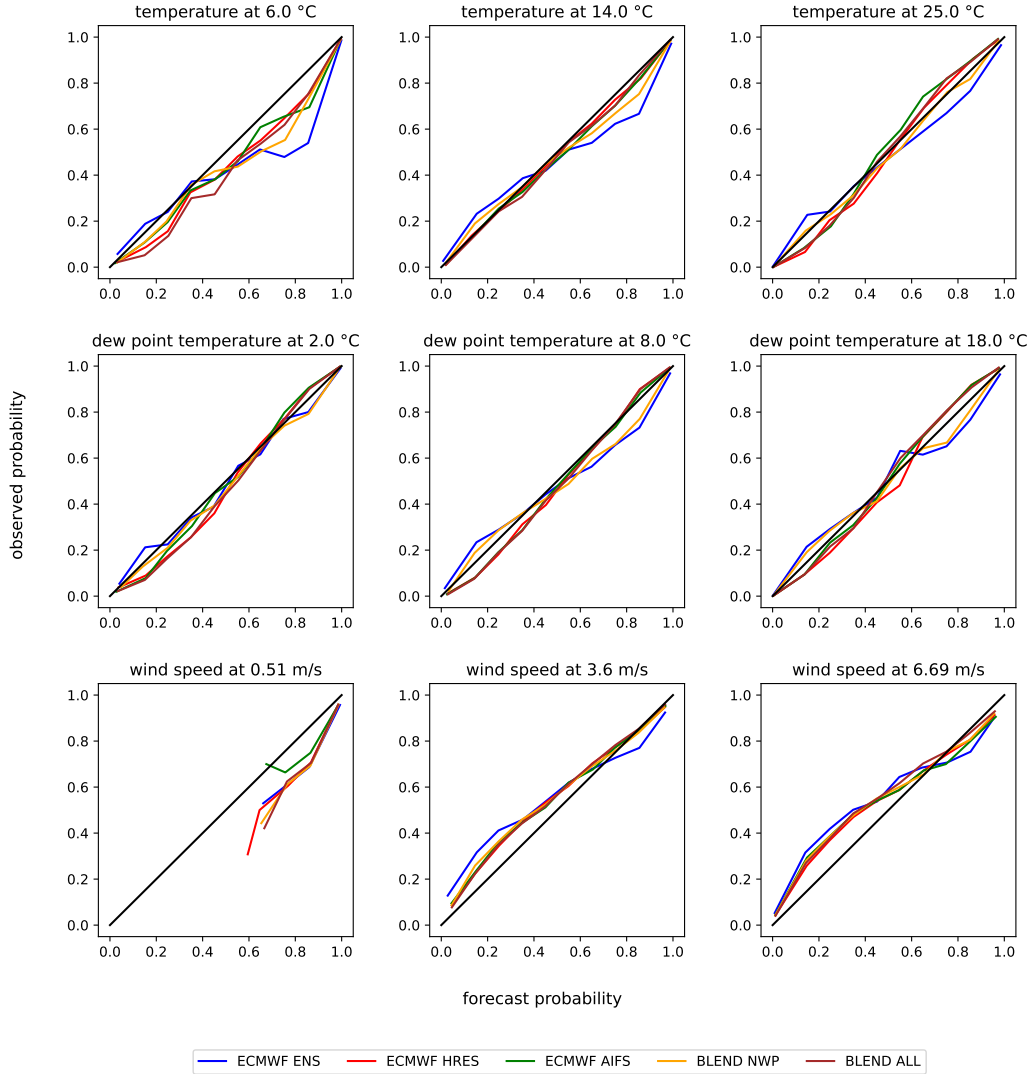


FIG. 10: Reliability at the 12-hour lead time for post-processed models ENS (blue), HRES (red), and AIFS (green), and blends (NWP models ENS and HRES, yellow; and all models, brown). Forecast probabilities are binned into 10 equal-width bins, and, for each bin, the average forecast and observed probability of exceeding the threshold is calculated. These values are linearly interpolated to produce the reliability curve. Bins having fewer than 10 data points are not plotted.

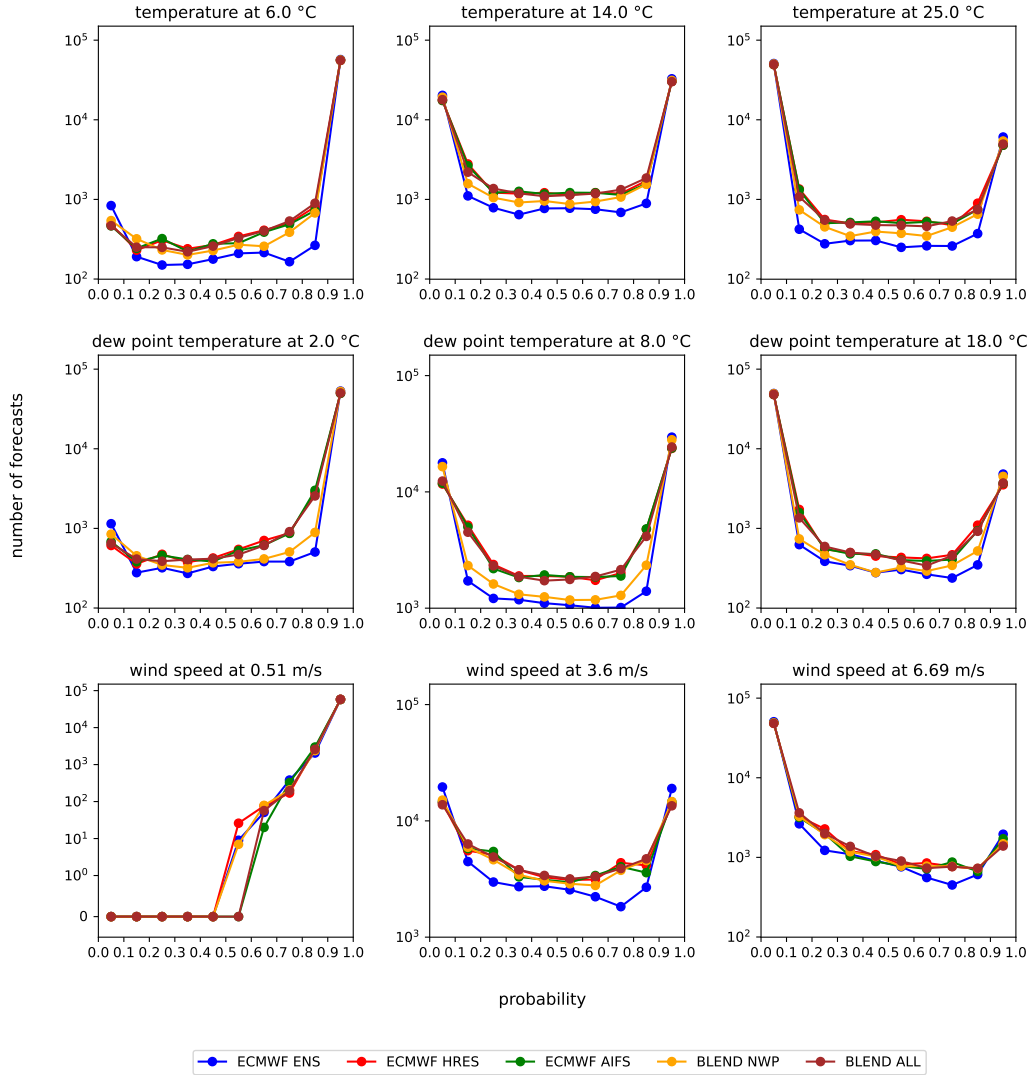


FIG. 11: Distribution of binned forecasts at the 12-hour lead time for post-processed models ENS (blue), HRES (red), and AIFS (green), and blends (NWP models ENS and HRES, yellow; and all models, brown). The y-axis uses the symmetric log scale, which is linear for values between 0 and 1, and logarithmic for larger values.

**Acknowledgments.** We wish to acknowledge ECMWF for making available data for the deterministic, ensemble, and AI forecasts; and the National Computing Infrastructure (NCI) Australia for providing the computing facilities used for this analysis. We are grateful to the UK Met Office for their contributions to the IMPROVER partnership. We thank Timothy Hume for contributions to the IMPROVER implementation at the Bureau, and for feedback on this paper. We also thank Mengmeng Han and Nicholas Loveday for useful feedback on a draft of this work.

**Data availability statement.** Data for the raw AIFS, ENS, and HRES forecasts is available from ECMWF via the MARS API. The open-source IMPROVER post-processing software is available from <https://github.com/metoppy/improver/>.

## References

- Ben Bouall  gue, Z., and Coauthors, 2024: The rise of data-driven weather forecasting: A first statistical assessment of machine learning-based weather forecasts in an operational-like context. *Bulletin of the American Meteorological Society*, **105** (6), E864–E883, <https://doi.org/10.1175/BAMS-D-23-0162.1>.
- Bi, K., L. Xie, H. Zhang, X. Chen, X. Gu, and Q. Tian, 2022: Pangu-weather: A 3d high-resolution model for fast and accurate global weather forecast. 2211.02556.
- Bremnes, J., T. Nipen, and I. Seierstad, 2024: Evaluation of forecasts by a global data-driven weather model with and without probabilistic post-processing at norwegian stations. *Nonlinear Processes in Geophysics*, **31** (2), 247–257, <https://doi.org/10.5194/npg-31-247-2024>.
- B  lte, C., N. Horat, J. Quinting, and S. Lerch, 2025: Uncertainty quantification for data-driven weather models. *Artificial Intelligence for the Earth Systems*, <https://doi.org/10.1175/AIES-D-24-0049.1>.
- de Burgh-Day, C. O., and T. Leeuwenburg, 2023: Machine learning for numerical weather and climate modelling: a review. *Geoscientific Model Development*, **16** (22), 6433–6477, <https://doi.org/10.5194/gmd-16-6433-2023>.
- ECMWF, 2025a: Atmospheric model high resolution 15-day forecast (set i - hres). URL <https://www.ecmwf.int/en/forecasts/datasets/set-i>.
- ECMWF, 2025b: Implementation of AIFS Single v1. URL <https://confluence.ecmwf.int/display/FCST/Implementation+of+AIFS+Single+v1>.
- Flowerdew, J., 2014: Calibrating ensemble reliability whilst preserving spatial structure. *Tellus A: Dynamic Meteorology and Oceanography*, **66** (1), 22 662, <https://doi.org/10.3402/tellusa.v66.22662>.
- Ge, T., J. Pathak, A. Subramaniam, and K. Kashinath, 2022: DL-Corrector-Remapper: A grid-free bias-correction deep learning methodology for data-driven high-resolution global weather forecasting. URL <https://arxiv.org/abs/2210.12293>, 2210.12293.
- Glowacki, T. J., Y. Xiao, and P. Steinle, 2012: Mesoscale Surface Analysis System for the Australian domain: Design issues, development status, and system validation. *Weather and Forecasting*, **27** (1), 141–157, <https://doi.org/10.1175/WAF-D-10-05063.1>.
- Henzi, A., J. F. Ziegel, and T. Gneiting, 2021: Isotonic distributional regression. *Journal of the Royal Statistical Society Series B: Statistical Methodology*, **83** (5), 963–993, <https://doi.org/10.1111/rssb.12450>.
- Hering, A. S., and M. G. Genton, 2011: Comparing spatial predictions. *Technometrics*, **53** (4), 414–425, <https://doi.org/10.1198/TECH.2011.10136>.
- Keisler, R., 2022: Forecasting global weather with graph neural networks. URL <https://arxiv.org/abs/2202.07575>, 2202.07575.
- Lam, R., and Coauthors, 2023: Learning skillful medium-range global weather forecasting. *Science*, **382** (6677), 1416–1421, <https://doi.org/10.1126/science.adi2336>.
- Lang, S., and Coauthors, 2024a: AIFS – ECMWF’s data-driven forecasting system. URL <https://arxiv.org/abs/2406.01465>, 2406.01465.
- Lang, S., and Coauthors, 2024b: AIFS-CRPS: Ensemble forecasting using a model trained with a loss function based on the Continuous Ranked Probability Score. URL <https://arxiv.org/abs/2412.15832>, 2412.15832.
- Leeuwenburg, T., and Coauthors, 2024: scores: A Python package for verifying and evaluating models and predictions with xarray. *Journal of Open Source Software*, **9** (99), 6889, <https://doi.org/10.21105/joss.06889>.
- Loveday, N., and Coauthors, 2024: The Jive verification system and its transformative impact on weather forecasting operations. *Bulletin of the American Meteorological Society*, **105** (11), E2047 – E2063, <https://doi.org/10.1175/BAMS-D-23-0267.1>.
- Owen, B., and Coauthors, 2024: An initial benchmarking of IMPROVER - Part 1: evaluation of non-precipitation diagnostics. *Bureau of Meteorology Research Report 092*.
- Owen, B., and Coauthors, 2025: Improving post-processing of deterministic models via fuzzy thresholding – a report on IMPROVER Release 6. *Bureau of Meteorology Research Report 112 (to appear)*.
- Ranjan, R., and T. Gneiting, 2010: Combining probability forecasts. *Journal of the Royal Statistical Society Series B: Statistical Methodology*, **72**, 71–91, <https://doi.org/10.1111/j.1467-9868.2009.00726.x>.
- Roberts, N., and Coauthors, 2023: IMPROVER: The new probabilistic postprocessing system at the met office. *Bulletin of the American Meteorological Society*, **104** (3), E680 – E697, <https://doi.org/10.1175/BAMS-D-21-0273.1>.
- Walz, E.-M., A. Henzi, J. Ziegel, and T. Gneiting, 2024: Easy uncertainty quantification (EasyUQ): Generating predictive distributions from single-valued model output. *SIAM Review*, **66** (1), 91–122, <https://doi.org/10.1137/22M1541915>.
- Wu, X., A. Ajorlou, Z. Wu, and A. Jadbabaie, 2023: Demystifying over-smoothing in attention-based graph neural networks. *37th Conference on Neural Information Processing Systems*, NeurIPS.